Supplementary Information

Distinct ferrovalley characteristic for Janus RuClX (X = F, Br) monolayer

Yubiao Ma[a], Yanzhao Wu[a], Junwei Tong[b], Li Deng[a], Xiang Yin[a], Lianqun Zhou[c], Xiaoli Han[d], Fubo Tian[e], and Xianmin Zhang[a]*

[a]Key Laboratory for Anisotropy and Texture of Materials (Ministry of Education), School of Material Science and Engineering, Northeastern University, Shenyang, 110819, China

[b]Department of Physics, Freie Universität Berlin, Berlin, 14195, Germany

[c]Suzhou Institute of Biomedical Engineering and Technology, Chinese Academy of Sciences, Suzhou 215163, China

[d]Taian Weiye Electromechanical Technology Co., Ltd, Taian, 271000, China

[e]State Key Laboratory of Superhard Materials, College of Physics, Jilin University, Changchun, 130012, China

Figures S1(a) and S1(b) show the spin charge density distribution of RuClF and RuClBr monolayers with FM and AFM states, respectively. It can be seen that the spin charge density of both spin-up (yellow in Figures S1) and spin-down (cyan in Figures S1) orientations is mainly concentrated on the Ru atoms, while the spin charge density of Cl, F or Br atoms are small enough to be neglected. This proves that the moment of RuClX monolayer is mainly contributed by the Ru atoms.
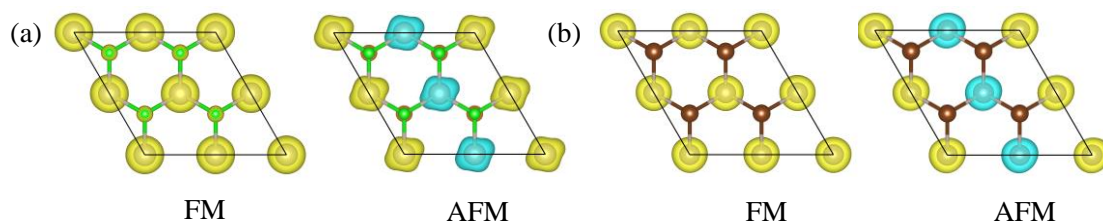
Figure S1. The spin charge density of the FM and AFM states for (a) RuClF and (b) RuClBr monolayers, respectively. The yellow and cyan represent spin up and spin down charge density, respectively. The isovalue is 0.04 e/Bohr^3.

Figures S2(a) and (b) show the projected density of states of Ru-d, Cl-p and F/Br-p orbitals in RuClF and RuClBr monolayers. It is found that d_{xy} and $d_{x^2-y^2}$, d_{xz} and d_{yz}, p_x and p_y orbitals are degenerate. By comparing Figure S2(a) and Figure S2(b), it can be found that the strength of the unoccupied states (at the energy positive of 1 eV) d_{z^2} orbitals is smaller in Figure S2(b). Thus, the interaction between the occupied spin-up states of d_{yz} and the unoccupied spin-down states of d_{z^2} orbitals in RuClBr monolayer would generate a smaller out-of-plane magnetic anisotropy.
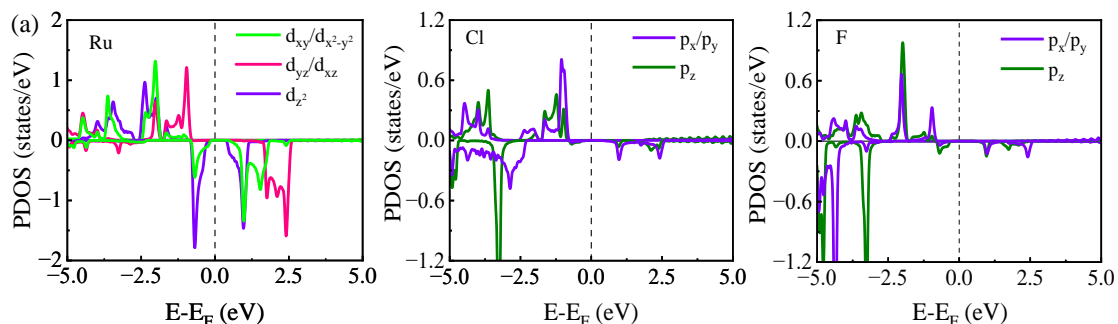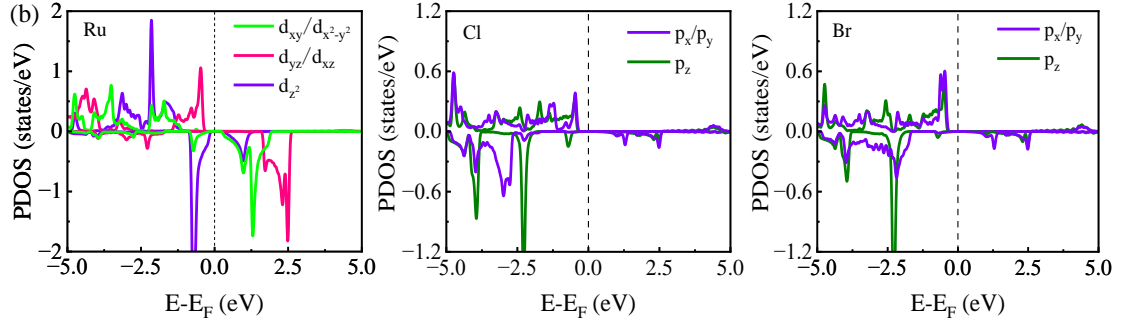
Figure S2. (a) The projected density of states (PDOS) of Ru, Cl and F atoms in RuClF monolayer. (b) The PDOS of Ru, Cl and Br atoms in RuClBr monolayer. Fermi energy level is set to zero.

Figures S3(a)-S3(e) show the d-orbitals projected band structures of Ru atoms in the RuClF monolayer. As shown in Figures S3(a) and S3(e), the valley states at the K and K′ points are mainly contributed by the occupied d_{xy} and $d_{x^2-y^2}$ orbitals of Ru atoms. The d_{z^2} orbitals of Ru atoms are mainly distributed near the K and K′ points of the conduction band, as displayed in Figure S3(c).
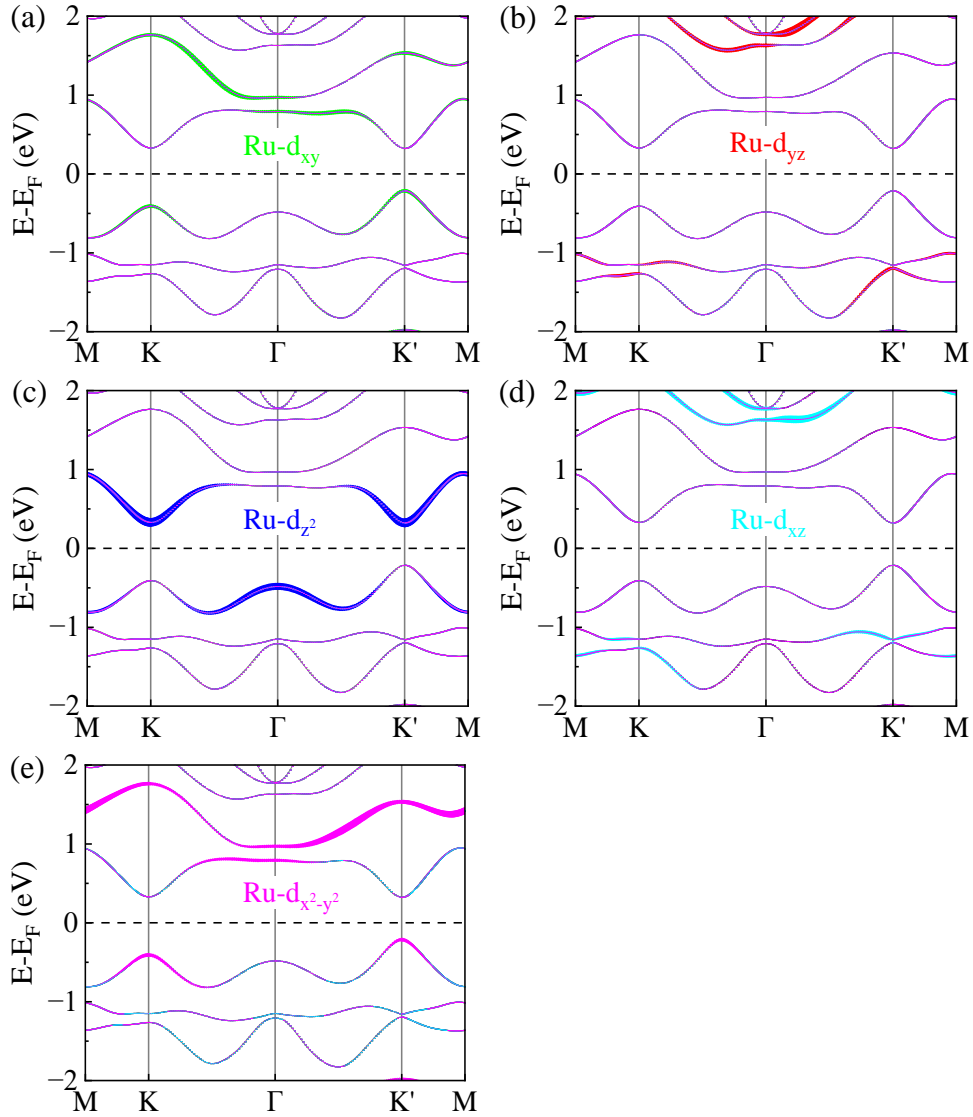
Figure S3. (a)-(e) Projected band structures of Ru-d orbitals for the RuClF monolayer. Fermi energy level is set to zero.

Figure S4(a)-S4(e) show the d-orbitals projected band structures of Ru atom in the RuClBr monolayer. From Figures S4(a) and S4(e), it is found that the valley states at the K and K′ points are mainly contributed by the unoccupied d_{xy} and $d_{x^2-y^2}$ orbitals of Ru atoms. As shown in Figure S4(c), the d_{z^2} orbitals of Ru atoms are mainly distributed near the K and K′ points of the valence band.
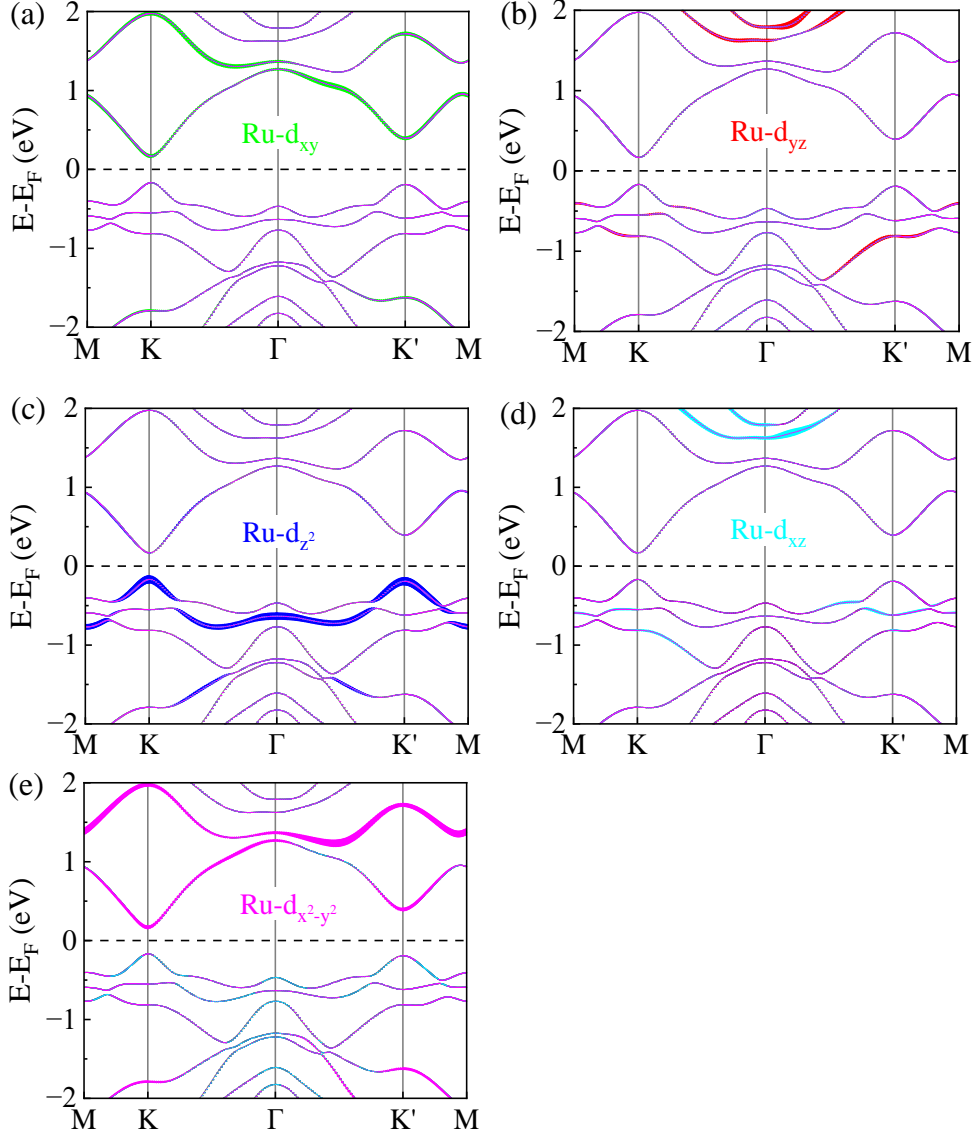
Figure S4. (a)-(e) Projected band structures of Ru-d orbitals for the RuClBr monolayer. Fermi energy level is set to zero.

The 4d orbitals of Ru atom, the 2p orbitals of F atom, the 3p orbitals of Cl atom, and 4p orbitals of Br atom are considered as the projected orbitals in calculating Wannier functions for the present RuClF and RuClBr monolayers, respectively. The corresponding parameters of the frozen and outer energy windows for Wannier fitting are list in Table S1.

Table S1. The parameters of the frozen and outer energy windows for Wannier fitting.

System	Frozen energy windows (eV)	Outer energy windows (eV)
RuClF	-10.50, -1.98	-12.0, 2.0
RuClBr	-8.90, -1.0	-9.30, 8.0

Figure S5 presents the calculated data by the VASP method and the fitting results using

WANNIER functions for RuClF and RuClBr monolayers. It can be seen that the WANNIER fitted band structures are nearly identical with the VASP calculated results.
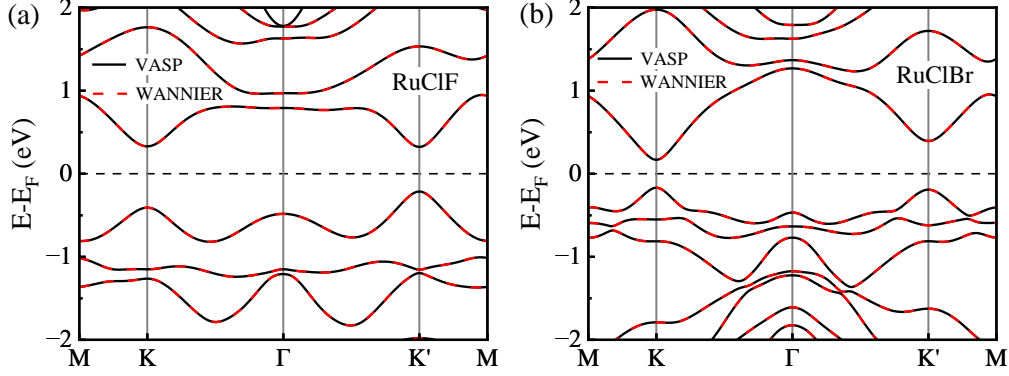
Figure S5. The calculated data by the VASP method and the fitting results using WANNIER functions for (a) RuClF and (b) RuClBr monolayers.

Figure S6 shows the final Wannier spread for each of wave function for RuClF monolayer. The Wannier spread for each of wave function is smaller than the lattice constant. The optimized lattice constant of RuClF monolayer is 3.34 Å.

```
Final State
 WF centre and spread    1  (  0.000001,  0.000180,-11.602537 )      0.89308211
 WF centre and spread    2  (  0.000001,  0.001903,-11.619107 )      1.08020221
 WF centre and spread    3  (  0.000001, -0.001055,-11.611377 )      0.88166220
 WF centre and spread    4  (  0.000003, -0.005065,-11.630551 )      1.16104057
 WF centre and spread    5  (  0.000001,  0.001058,-11.611375 )      0.88161185
 WF centre and spread    6  (  0.000001,  0.005087,-11.630554 )      1.16093300
 WF centre and spread    7  (  0.000000, -0.046873,-11.607261 )      0.91706057
 WF centre and spread    8  (  0.000001, -0.105075,-11.621500 )      1.20804216
 WF centre and spread    9  (  0.000000,  0.046605,-11.607258 )      0.91709940
 WF centre and spread   10  ( -0.000001,  0.102713,-11.621476 )      1.20879943
 WF centre and spread   11  ( -0.000003,  1.925647,-10.341487 )      0.59824342
 WF centre and spread   12  ( -0.000003,  1.925687,-10.338726 )      0.60468571
 WF centre and spread   13  (  0.000012,  1.937572,-10.367278 )      0.63620621
 WF centre and spread   14  (  0.000012,  1.936781,-10.362392 )      0.62871263
 WF centre and spread   15  ( -0.000002,  1.913677,-10.367278 )      0.63621039
 WF centre and spread   16  ( -0.000002,  1.914503,-10.362398 )      0.62875026
 WF centre and spread   17  ( -0.000004,  1.925707, 10.233828 )      1.41587931
 WF centre and spread   18  ( -0.000005,  1.925909, 10.217947 )      1.42087307
 WF centre and spread   19  (  0.000004,  1.939550, 10.249597 )      1.31243121
 WF centre and spread   20  (  0.000005,  1.942181, 10.236011 )      1.30918615
 WF centre and spread   21  ( -0.000003,  1.911679, 10.249595 )      1.31244779
 WF centre and spread   22  ( -0.000004,  1.909105, 10.236010 )      1.30920922
 Sum of centres and spreads (  0.000013, 23.107477,********** )     22.12236888
```

Figure S6. The final Wannier spread for each of wave function for RuClF monolayer.

Figure S7 shows the final Wannier spread for each of wave function for RuClBr monolayer. The Wannier spread for each of wave function is smaller than the lattice constant. The optimized lattice constant of RuClBr monolayer is 3.66 Å.

```
Final State
 WF centre and spread    1  (  0.000000,  0.000057, 11.681388 )      0.96537273
 WF centre and spread    2  (  0.000001,  0.000203, 11.683048 )      1.09302935
 WF centre and spread    3  (  0.000001, -0.007088, 11.688042 )      0.94655624
 WF centre and spread    4  (  0.000001, -0.012083, 11.700482 )      1.23992672
 WF centre and spread    5  (  0.000000,  0.007088, 11.688039 )      0.94641136
 WF centre and spread    6  (  0.000000,  0.012080, 11.700483 )      1.23968387
 WF centre and spread    7  (  0.000000, -0.040588, 11.682123 )      0.95732745
 WF centre and spread    8  (  0.000001, -0.090871, 11.685562 )      1.32573392
 WF centre and spread    9  (  0.000000,  0.040463, 11.682122 )      0.95733716
 WF centre and spread   10  (  0.000000,  0.090251, 11.685556 )      1.32589401
 WF centre and spread   11  ( -0.000006,  2.114131, 10.124889 )      1.36969418
 WF centre and spread   12  ( -0.000004,  2.114212, 10.119799 )      1.38526594
 WF centre and spread   13  (  0.000005,  2.139114, 10.181995 )      1.39106285
 WF centre and spread   14  (  0.000005,  2.140306, 10.170200 )      1.37824615
 WF centre and spread   15  ( -0.000004,  2.088914, 10.181994 )      1.39107555
 WF centre and spread   16  ( -0.000004,  2.087798, 10.170198 )      1.37827961
 WF centre and spread   17  ( -0.000004,  2.114181,-10.087780 )      1.73742665
 WF centre and spread   18  ( -0.000004,  2.114263,-10.078330 )      1.75165003
 WF centre and spread   19  (  0.000004,  2.138787,-10.127120 )      1.72192726
 WF centre and spread   20  (  0.000004,  2.141363,-10.111972 )      1.71407209
 WF centre and spread   21  ( -0.000003,  2.089195,-10.127117 )      1.72196884
 WF centre and spread   22  ( -0.000003,  2.086722,-10.111967 )      1.71414369
 Sum of centres and spreads ( -0.000010, 25.368499,117.181634 )     29.65208566
```

Figure S7. The final Wannier spread for each of wave function for RuClBr monolayer.

As observed in Figure S8(a), with 0.05 holes per f.u. are doped, the Fermi energy level passes

through the K′ valley in RuClF monolayer. Therefore, the carriers are dominated by the K′ valley. The Fermi energy level passes through the K valley in RuClBr monolayer with doping 0.05 electrons per f.u., as shown in Figure S8(b). At this time, the carriers are excited by the K valley. In the first-principles calculations, carrier doping is simulated by removing or adding electrons from the system and using a homogeneous background charge to maintain charge neutrality[1,2].
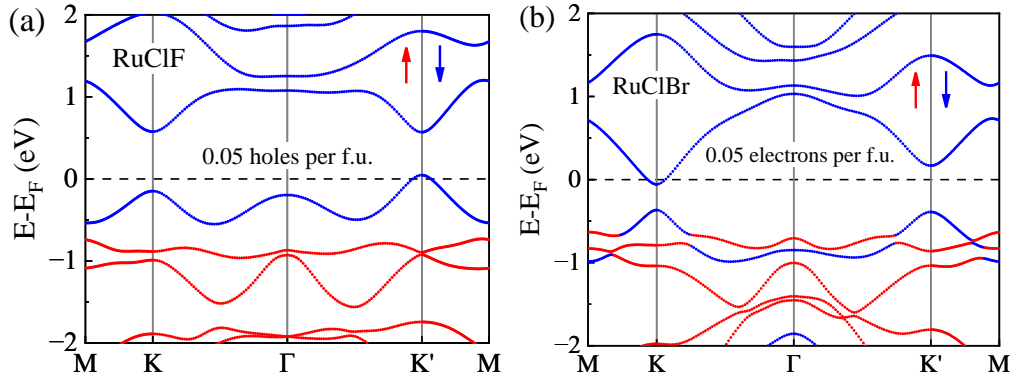
Figure S8. (a) The band structures with SOC of RuClF monolayer with doping 0.05 holes per f.u.. (b) The band structures with SOC of RuClBr monolayer with doping 0.05 electrons per f.u.. The red arrow represents spin up, and the blue arrow represents spin down. Fermi energy level is set to zero.

References

[1] X. Li, X. Wu, J. Yang, Half-Metallicity in MnPSe$_3$ Exfoliated Nanosheet with Carrier Doping, *Journal of the American Chemical Society*, **136** 11065 (2014).

[2] Y. Chen, Q. Fan, Y. Liu, G. Yao, Electrically tunable magnetism and unique intralayer charge transfer in Janus monolayer MnSSe for spintronics applications, *Physical Review B*, **105** 195410 (2022).